Behaviour of CVD diamond strip detectors in magnetic field

W. Adam, H. Pernegger
Institut für Hochenergiephysik d. Österr. Akademie d. Wissenschaften, Wien

October 28, 1996

1 Introduction

Diamond strip detectors based on CVD diamond material have been studied at high magnetic field. The detectors were tested in a 225 GeV/c pion beam at the CERN SPS accelerator. The diamond detectors, named F, DB26 and X, had 6.8 mm long strips with a pitch of 50 μm on one side and a continuous contact on the other side. Each strip was read out by a VA2 amplifier chip with an integration time of 1.8μs.

The diamond detectors were placed in the center of a reference telescope consisting of 4 planes of silicon strip detectors measuring the track co-ordinates transversal to the beam, x and y. Reference system and test detectors were located in the center of a superconducting magnet providing a field of up to 3T along the horizontal x co-ordinate. The strip orientation of the diamond detectors was parallel to the magnetic field. All detector planes were perpendicular to the beam axis. Figure 1 shows a schematic illustration of the test setup.

2 Reference system and event selection

The reference system was aligned using data taken at $B = 0T$. The diamond detectors, which were not used in the track fit, were aligned with respect to the reference system. These alignment parameters were subsequently used for the analysis of all data taken at magnetic fields of 0, 2 and 3T.

Events were selected requiring exactly one track measured in both co-ordinates of all reference planes. Tracks were reconstructed as straight lines. Events with noise hits and multiple tracks were rejected. Clusters were defined as a sequence of adjacent strips with a S/N ratio higher than 1.5. Only clusters with a total S/N higher than 5 were accepted. The same values were used both for diamond and silicon detectors. Clusters containing noisy strips were rejected. Diamonds were required to have exactly one cluster in order to be considered in the analysis.

Figure 2 shows the beam profile in the xy plane for the reference system and the part covered by each diamond. Horizontal gaps in the profile are due to noisy channels, which have been suppressed in the analysis. Diamonds F and X indicate good efficiency, diamond DB26 exhibits very low efficiency and is not considered in the following analysis. Figure 3 shows the reconstructed track slope for different values of the magnetic field. The magnetic field causes a slope of 4 and 6 mrad at a field of 2 and 3T respectively. The bottom plots show the residual distribution for the silicon reference planes 3 and 4 measureing the y co-ordinate. The Lorentz shift of the clusters is clearly visible in both reference planes. The sign of the shift is different, as the strip side of reference 3 was beam downstream and the strip side of reference 4 beam upstream, hence the electric field had opposite sign on the two detectors.

3 Diamond cluster parameters at different field

Clusters on the diamond detectors were reconstructed by applying the thresholds mentioned above to the strip signals. The clusters were required to be in a 0.5mm region on either side of the predicted hit position. Events with tracks outside the diamond's acceptance were rejected. Figure 4 shows distributions of cluster multiplity per event and cluster width on diamond F for fields of 0, 2 and 3T. The signals, measured by an ADC, were calibrated with pulses on a test capacitance, yielding calibration constants of 31.0 electrons / ADC count for diamond X and 26.6 electrons / ADC counts for diamond F. At the time of the measurements diamond F was in a pumped state, diamond X in a depumped state.

The signal distribution of diamond F, as shown in figure 5, remained essentially unchanged at all magnetic field values. The mean signal was about 3400 electrons, which corresponds to a collection distance of 94μm. On average the signal was contained in two strips. The uniformity of the signal over the diamond area has been verified. No regions of low signal were observed.

Figures 6 and 7 show the same distributions for diamond X. The signal is significantly smaller, on average 1600 electrons, and does not exhibit the expected Landau distribution. The clusters on diamond X are significantly wider than on diamond F. The mean signal corresponds to a collection distance of 44μm. The signal size is uniform over the detector area, no regions with an enhanced population of wider or narrower clusters could be found, indicating a uniform signal behaviour over the detector surface. Signal parameters for both diamonds are summarized in table 1.

4 Spatial resolution, signal shape and Lorentz shift

Tracks were reconstructed as straight lines between reference planes 1—4. The Lorentz shifts in the reference detectors were not taken into account. Since they had opposite signs in planes 1 and 2 respectively 3 and 4, and since the track slopes were small, reconstructed tracks were not systematically shifted in the reconstruction from their true position. Only the sagitta between the real, bended particle trajectory and the reconstructed straight line had to be taken into account. The bending radius R in m can be calculated as

$$R = 3.33 \frac{p}{Bq} \tag{1}$$

where p denotes the particle momentum transvers to the B-field in GeV/c, B the magnetic field in T and q the charge of the particle in units of the elementary charge. This yields a bending radius of 250m for B=3T and 375m for B=2T. The sagitta s between the real track and the reconstructed line is approximately

$$s = \frac{dz(L - dz)}{2R} \tag{2}$$

where L=180mm is the distance between the two sets of reference planes and dz the distance of the diamond detector to the first set reference planes (see figure 1).

The Lorentz shift of the clusters Δy in the diamond detectors can be obtained from the calculated sagitta plus the measured shift of the residual distribution with respect to the reconstructed straight line. Alternatively the position of the maximum signal can be measured with respect to the predicted hit position when the hit extrapolation is displaced by the expected sagitta. Both methods were used to determine the Lorentz shift of the clusters.

Figure 8 shows the residual distribution of diamond F for fields of 0, 2, and 3T. The resolution of 15.8μm is found to be constant within the measurement error. A clear shift of the residuals at 2 and 3 Tesla is visible. The measured Lorentz shift, after correction for the sagitta, is 24.8μm at 3 Tesla and shows a linear dependance on the magnetic field.

Figure 9 shows the residual distributions for diamond X. Diamond X exhibits a slightly worse resolution of 17.9μm than diamond F, but no significant change with magnetic field. The Lorentz shift is 18.1μm at 3 Tesla with the same type of dependance as for diamond F.

In the second analysis the signal shape and position were investigated at different values of the magnetic field. For this analysis the average signal of a single strip was plotted versus the predicted track position with respect to the strip center. This allows to study the spread of the signal under the influence of diffusion and magnetic field, the shift of the charge cloud as a result of the Lorentz force and a possible asymmetry of the measured charge cloud. As this analysis uses only the predicted hit position it is independent of thresholds.

Figure 10 shows the average strip signal versus the predicted hit position. The predicted hit position is calculated from the track extrapolation and the sagitta. The top plot gives the signal shape as projected on the plane perpendicular to the strips for diamond F at fields of 0, 2 and 3T. The measured points are fitted to a Gaussian distribution. It can be seen that both size and shape of the signal remain unchanged with the magnetic field. The width of the distribution, as given by the σ of the Gaussian fit, is 22μm. No asymmetry of the signal shape with respect to its center is observed. The Lorentz shifts are consistent with those measured in the first analysis.

The lower plot shows the signal shape for diamond X. Also for diamond X the shift of the cluster as a result of the Lorentz force increases with the magnetic field. No significant asymmetry beyond the statistical errors is observed. With a width ofσ=35μm clusters measured on diamond X are substantially wider than on diamond F, but do not change with the magnetic field.

Resolutions and Lorentz shifts for both diamonds and for all values of the magnetic field are shown in table 2.

5 Summary

The influence of magnetic field on signal and spatial resolution of diamond strip detectors has been studied. The magnetic field causes a shift of the clusters, which increases linearly with the magnetic field strength, but does not change spatial resolution, cluster signal or width. The Lorentz shift is found to be different for diamonds F and X, which may be related to the difference in collection distance. Figure 11 shows various detector parameters of diamonds F and X versus the magnetic field strength.

	diamond F			diamond X		
	B=0T	B=2T	B=3T	B=0T	B=2T	B=3T
mean signal (e^-)	3361.	3412.	3293.	1612.	1580.	1522.
most probable signal (e^-)	2242.	2284.	2193.	794.	756.	758.

Table 1: Mean and most probable signal in electrons for diamonds F and X at different values of the magnetic field.

	diamond F			diamond X		
	B=0T	B=2T	B=3T	B=0T	B=2T	B=3T
resolution (μm)	15.4	16.2	15.9	17.8	18.3	17.5
sagitta (μm)	0.0	10.0	15.0	0.0	6.8	10.2
Δy from residuals (μm)	0.0	16.7	24.8	0.0	12.1	18.1
Δy from charge distribution (μm)	0.0	16.2	24.3	0.0	12.5	17.3

Table 2: Resolution, sagitta of the track and Lorentz shift for diamonds F and X at different values of the magnetic field. The Lorentz shifts have been calculated using two different methods (see text).

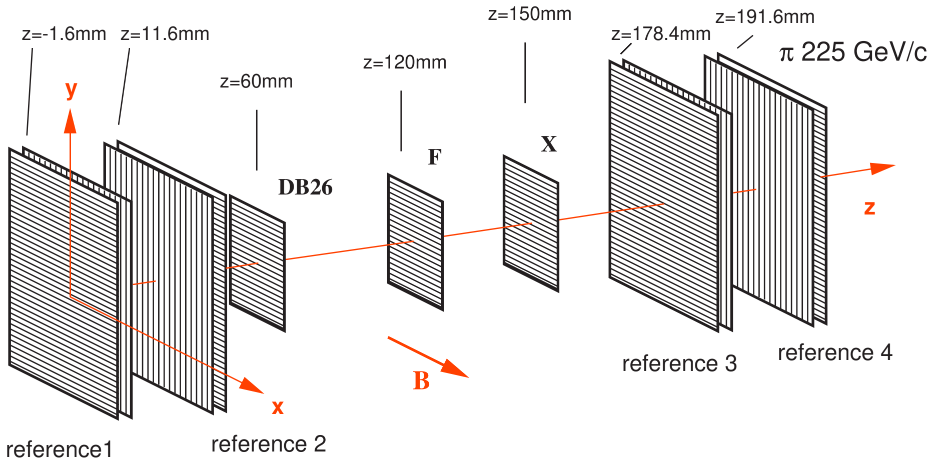

Figure 1: Test setup

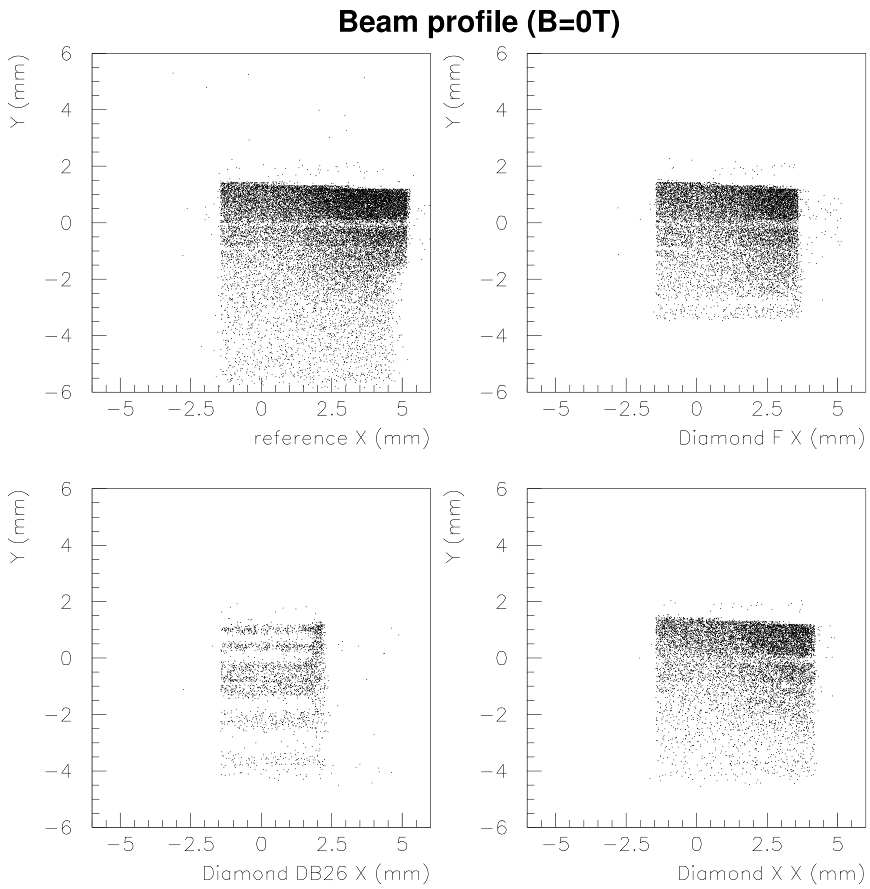

Figure 2: Beam profile in reference detectors and diamond detectors

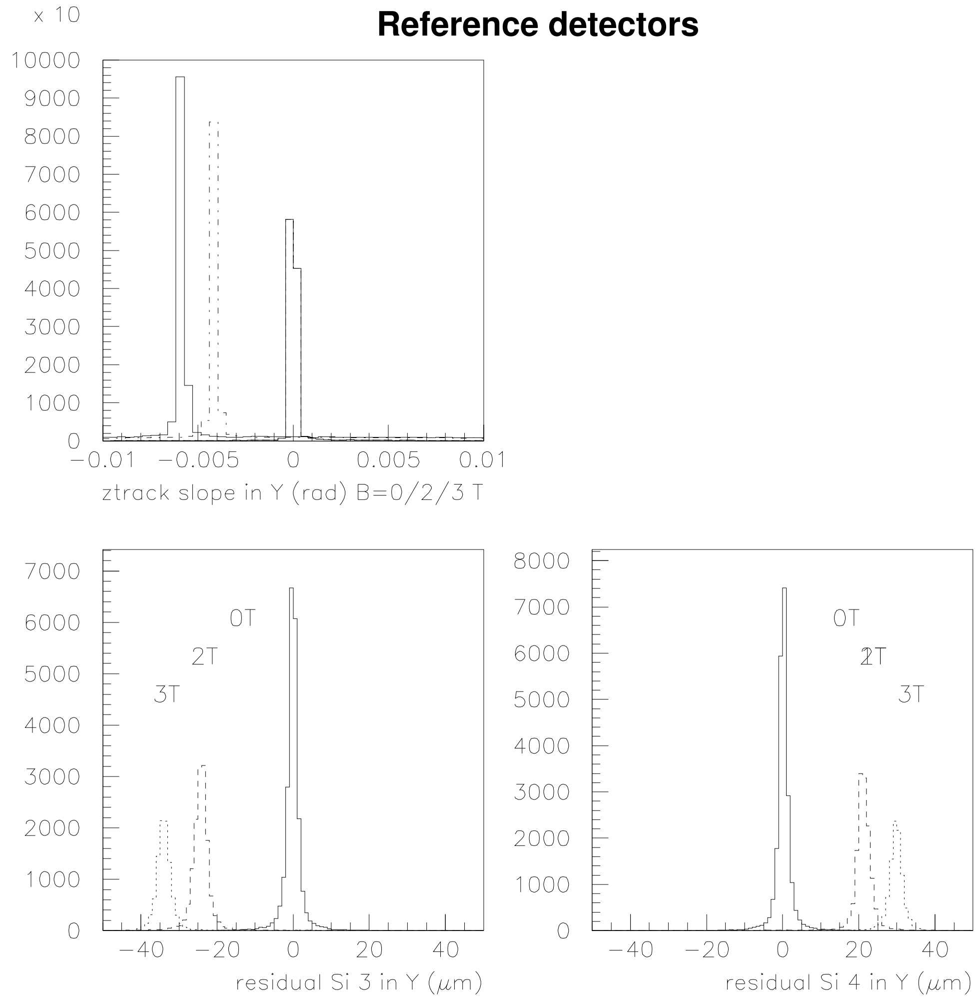

Figure 3: Track slope and residual distribution in the reference silicon detectors

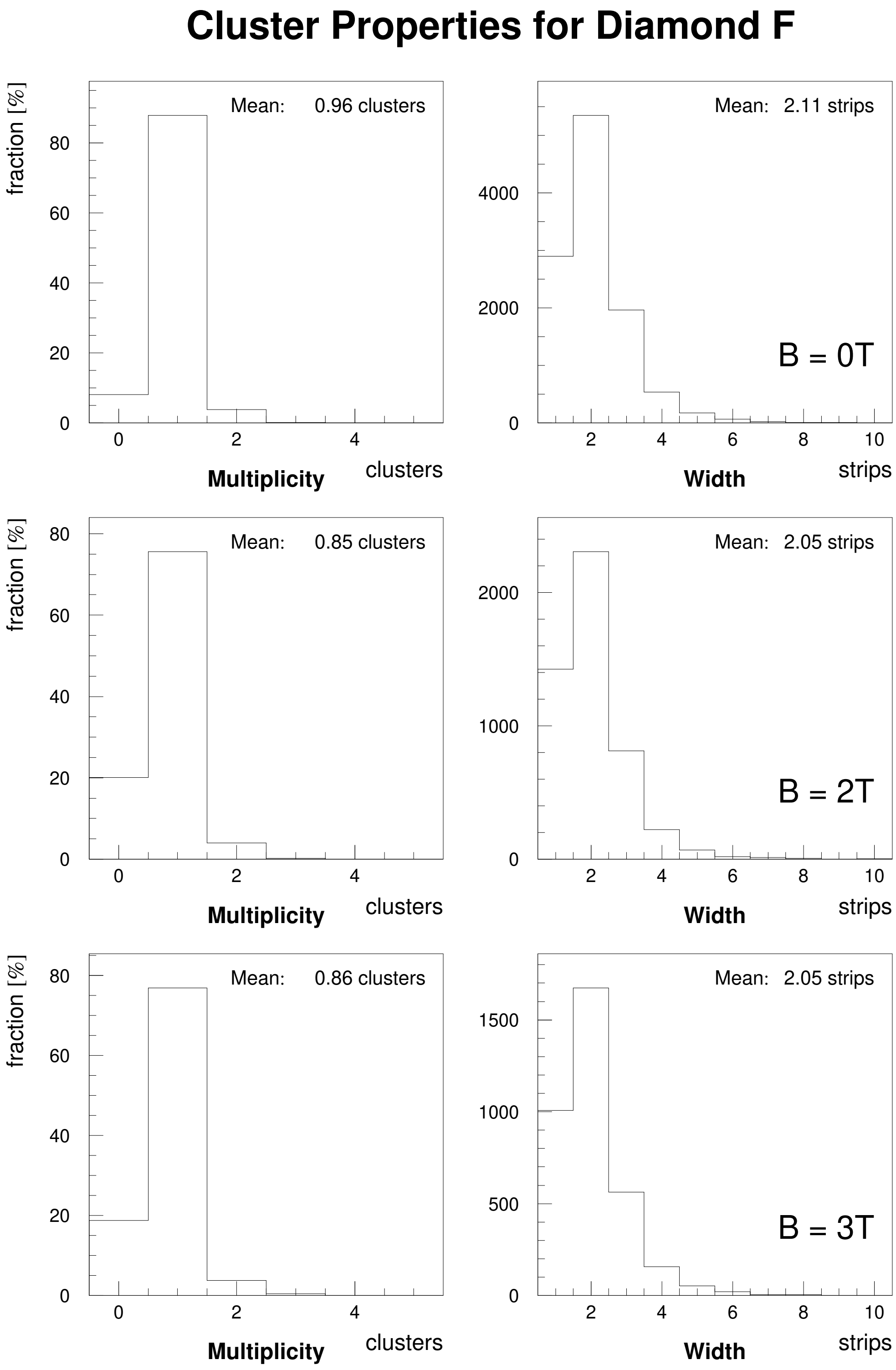

Figure 4: Cluster multiplities and cluster width for single cluster events at different values of the magnetic field for diamond F

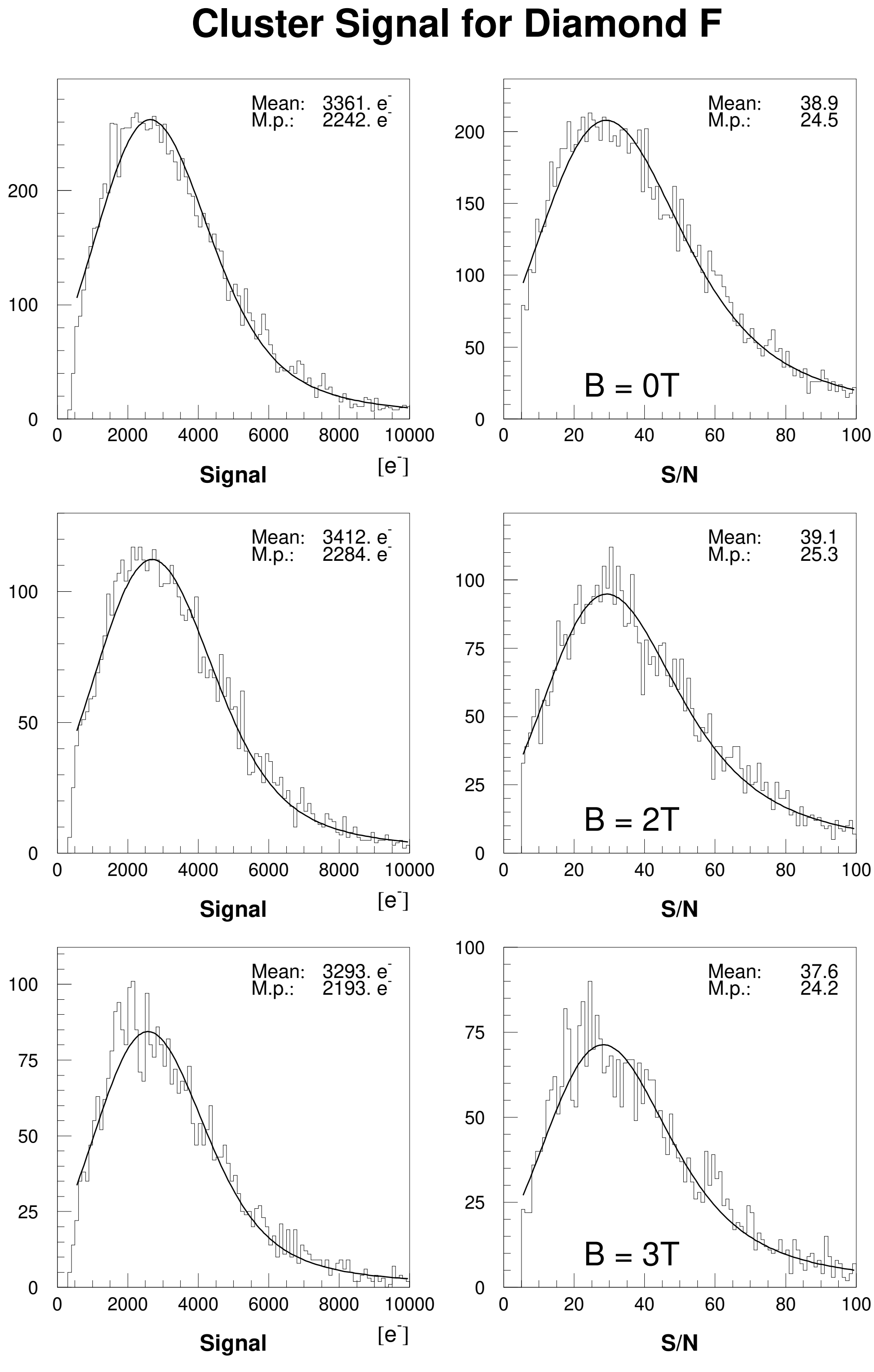

Figure 5: Cluster signal and S/N at different values of the magnetic field for diamond F

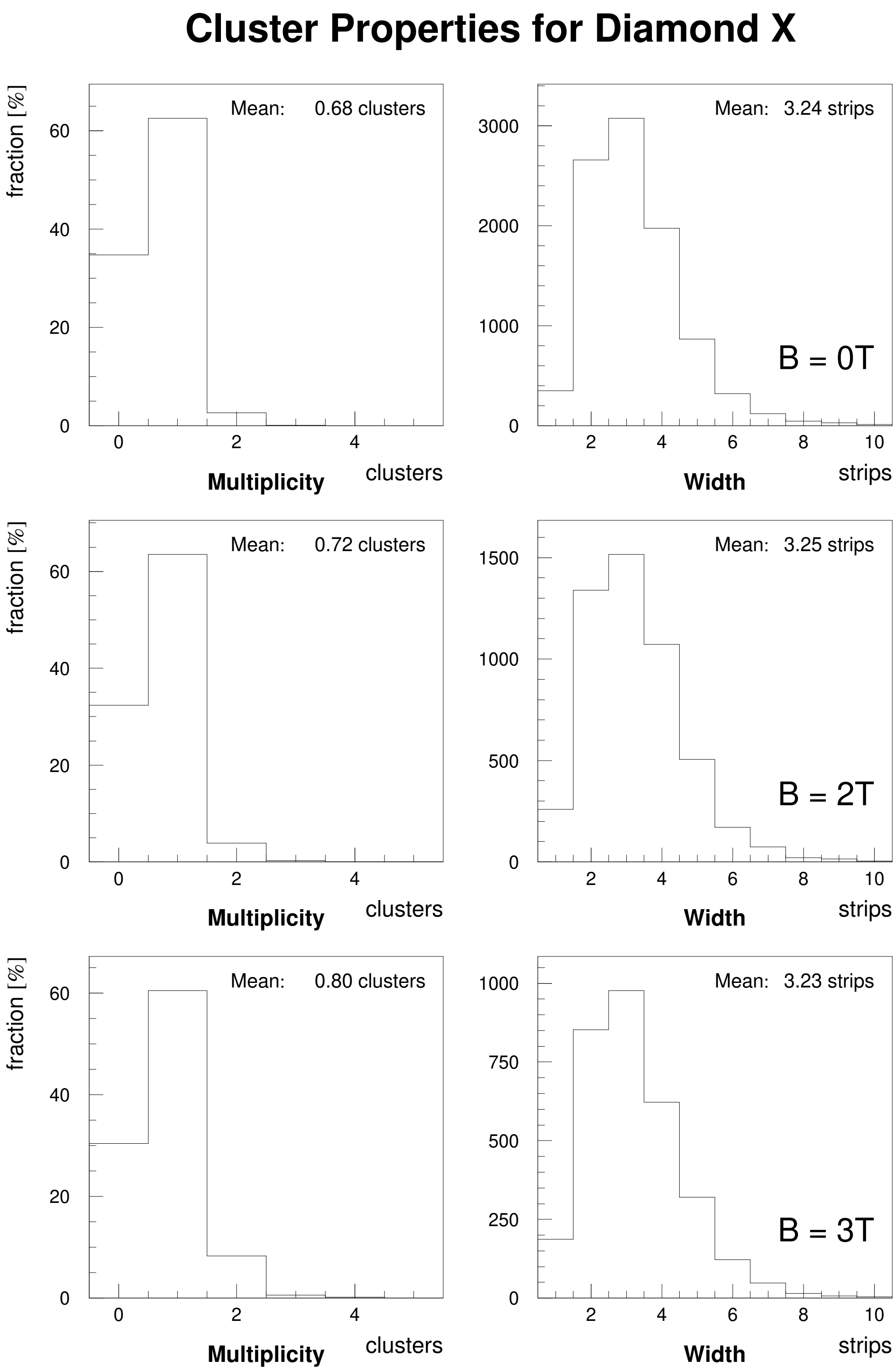

Figure 6: Cluster multiplities and width at different values of the magnetic field for diamond X

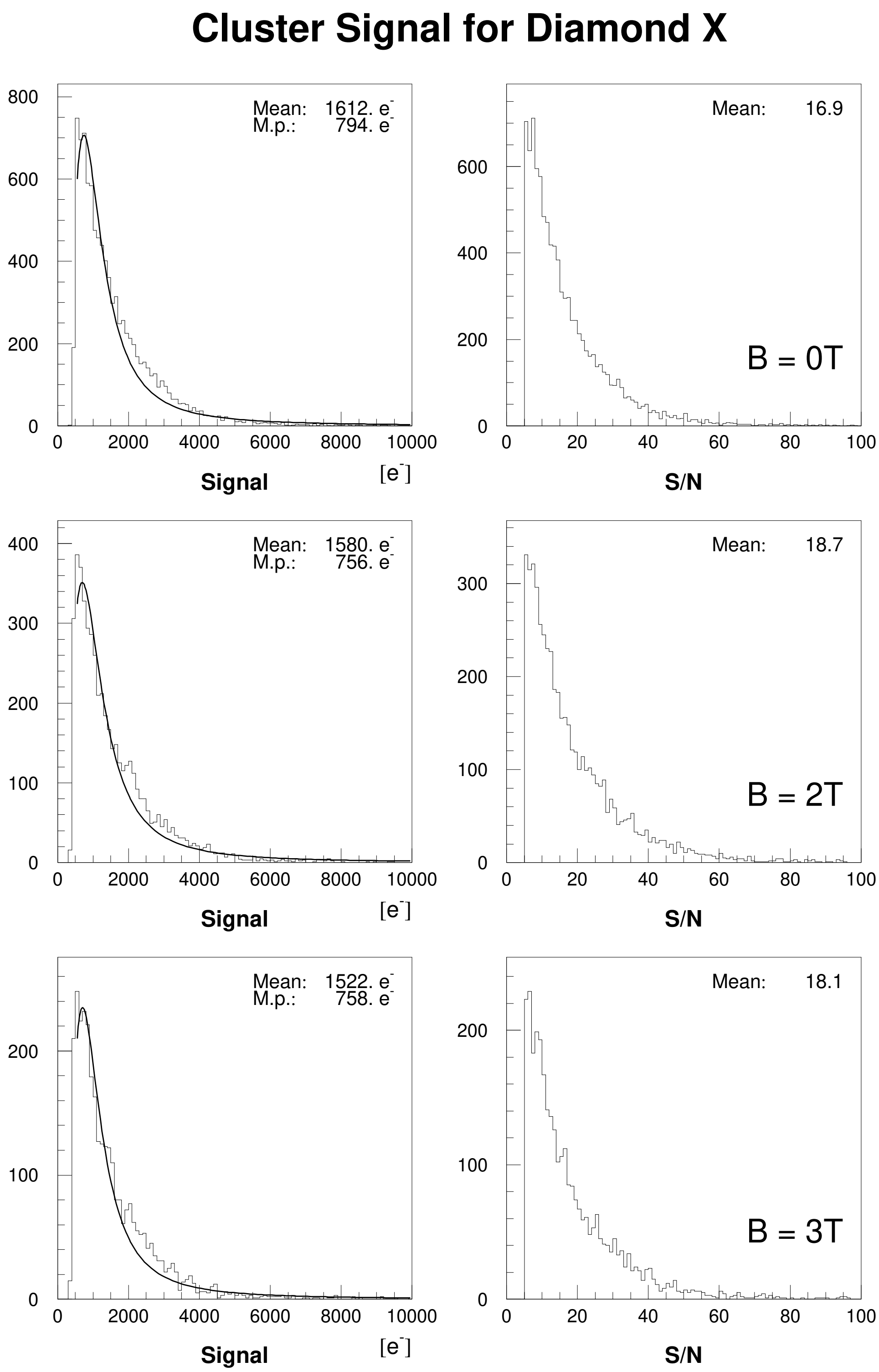

Figure 7: Cluster signal and S/N at different values of the magnetic field for diamond X

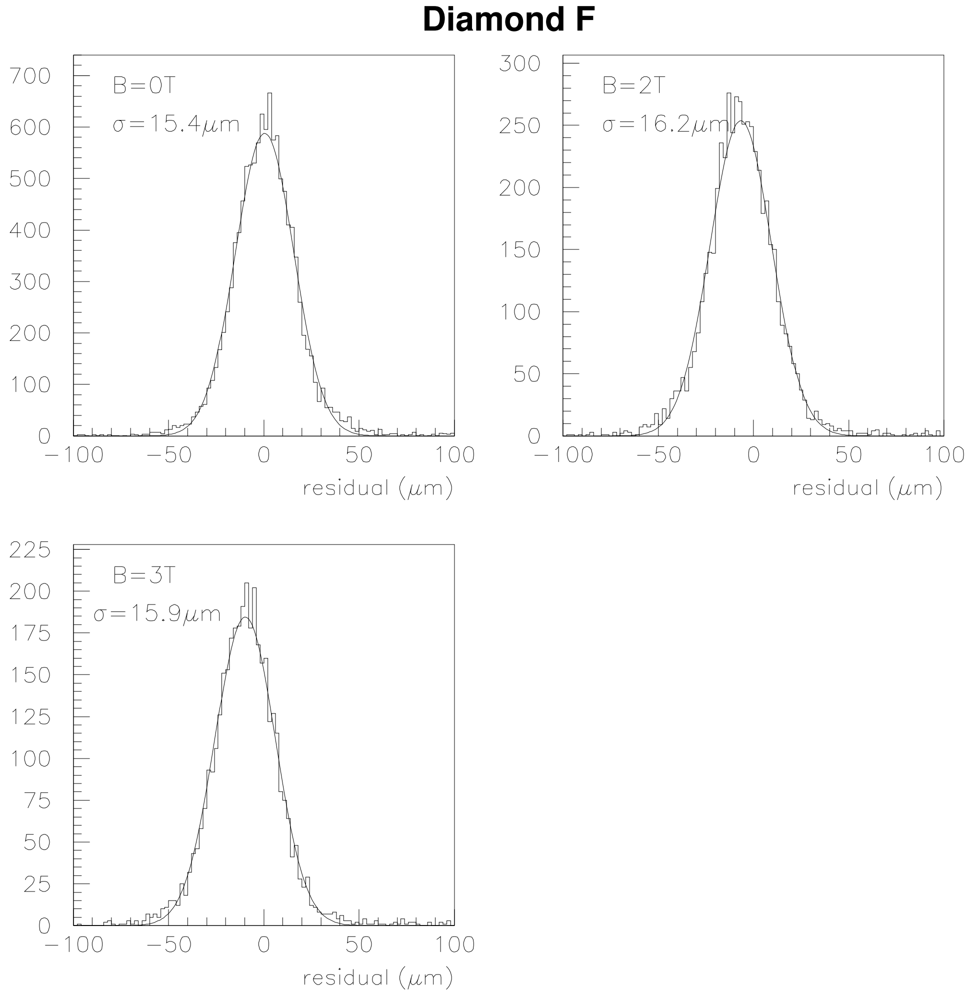

Figure 8: Residual distribution for diamond F at different magnetic field strength

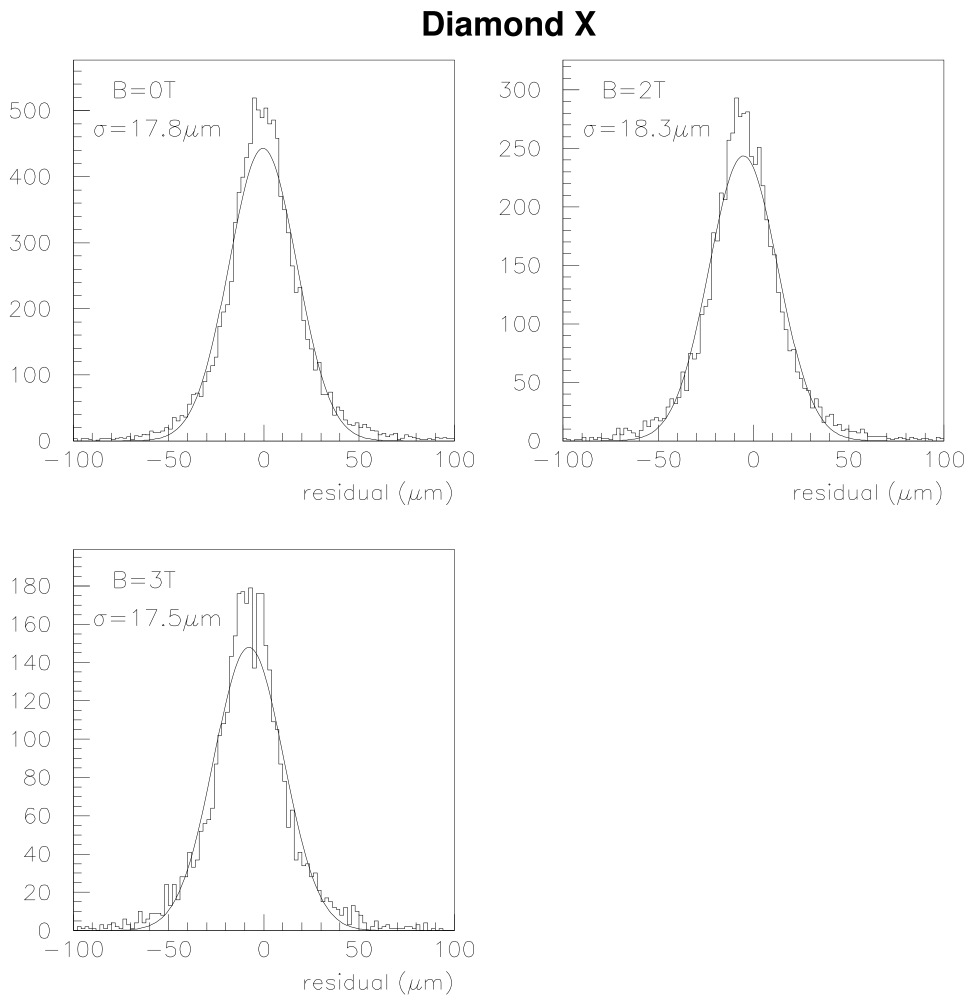

Figure 9: Residual distribution for diamond X at different magnetic field strength

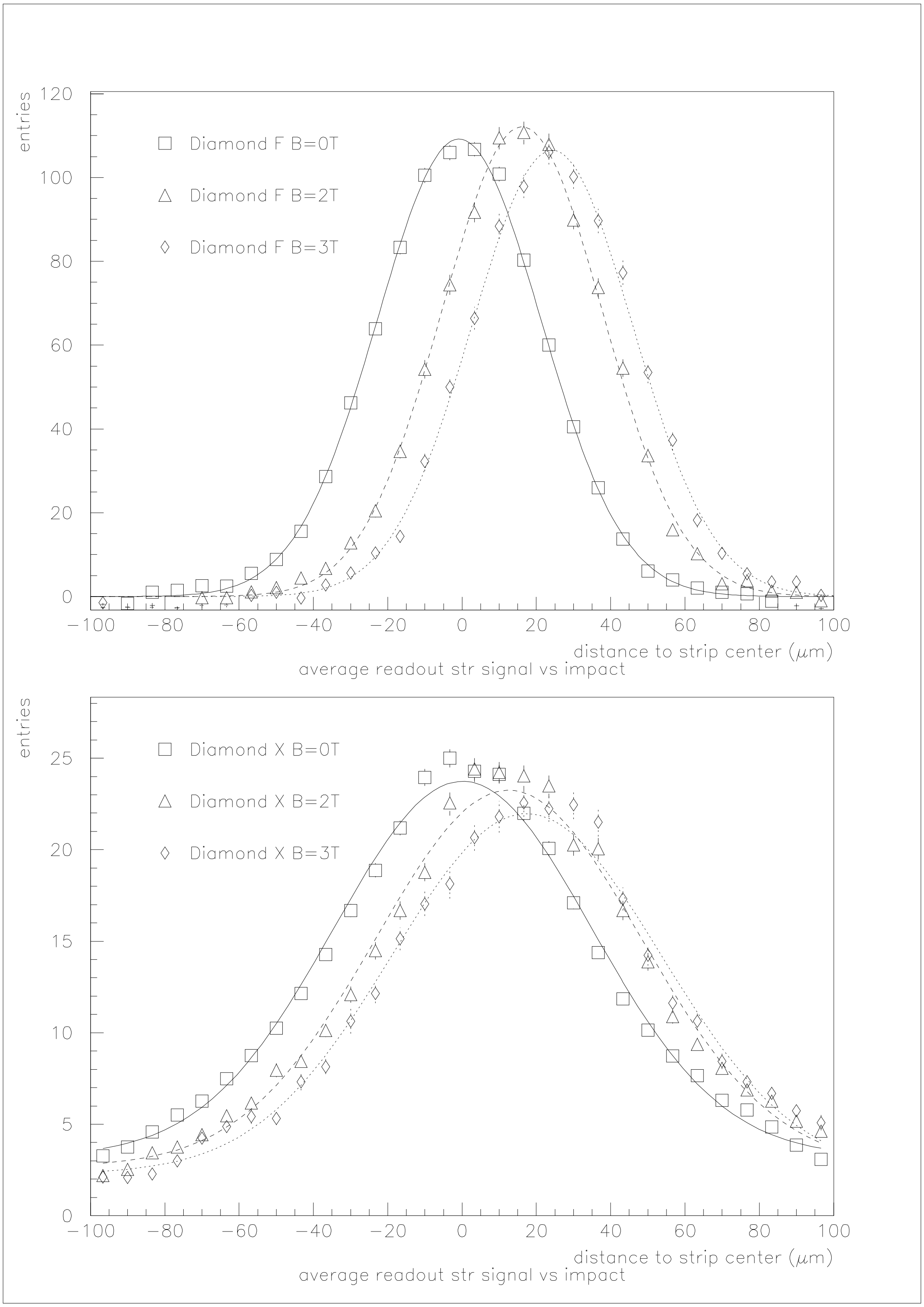

Figure 10: Signal shape for different values of magnetic field strength in diamond F and X

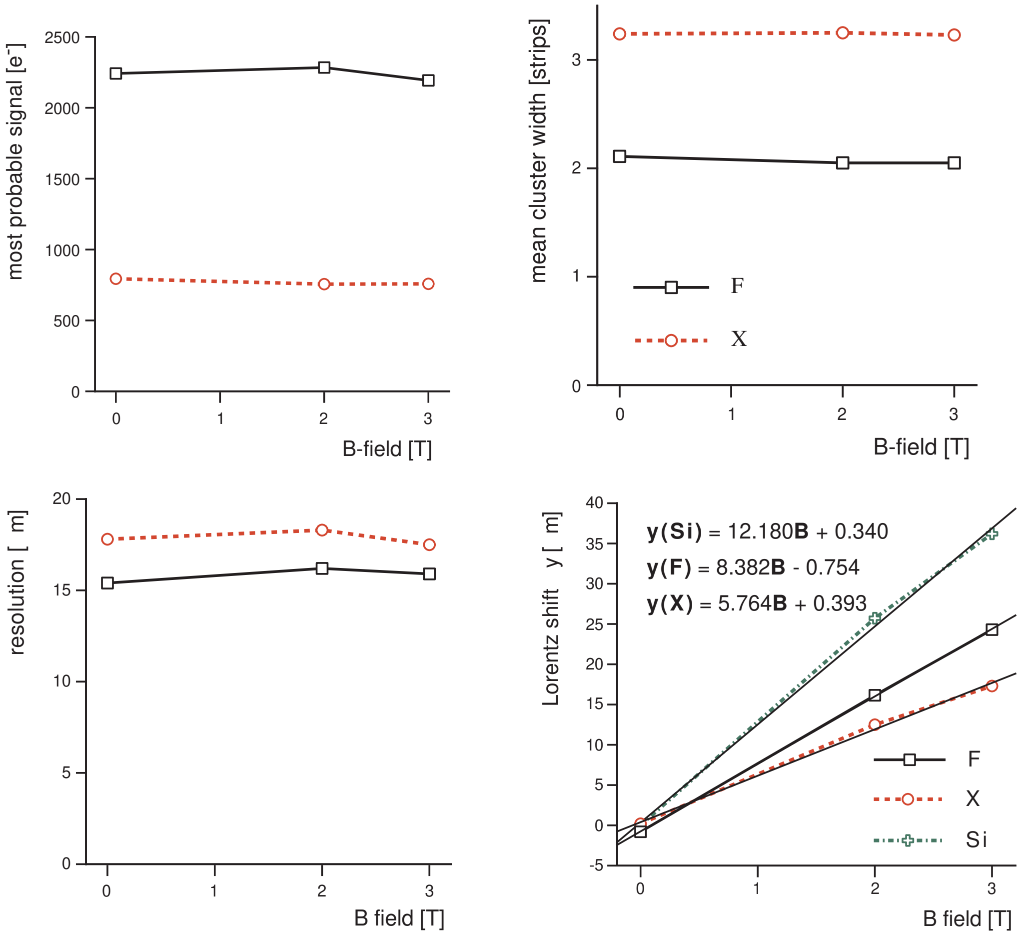

Figure 11: Mean cluster signal (top left), cluster width (top right, in units of readout pitch), spatial resolution (bottom left) and Lorentz shift (bottom right) at different values of the magnetic field. The Lorentz shift as measured on silicon strip detector reference Y3 is compared to the diamond data.